Title

A digital CDS technique and its performance testing

Journal

Chinese Physics C, 39(7)

ISSN

1674-1137

Authors

Liu, Xiao-Yan

Lu, Jing-Bin

Yang, Yan-Ji

et al.

Publication Date

2015-07-01

DOI

10.1088/1674-1137/39/7/076101

Peer reviewed

PAPER

A digital CDS technique and its performance testing

To cite this article: Liu Xiao-Yan *et al* 2015 *Chinese Phys. C* **39** 076101

A digital CDS technique and its performance testing*

LIU Xiao-Yan(刘晓艳)[1,2] LU Jing-Bin(陆景彬)[1] YANG Yan-Ji(杨彦佶)[1,2] LU Bo(陆波)[2]
WANG Yu-Sa(王于仨)[2] XU Yu-Peng(徐玉朋)[2] CUI Wei-Wei(崔苇苇)[2] LI Wei(李炜)[2]
LI Mao-Shun(李茂顺)[2] WANG Juan(王娟)[2] HAN Da-Wei(韩大炜)[2] CHEN Tian-Xiang(陈田祥)[2]
HUO Jia(霍嘉)[2] HU Wei(胡渭)[2] ZHANG Yi(张艺)[2] ZHU Yue(朱玥)[2] ZHANG Zi-Liang(张子良)[2]
YIN Guo-He(尹国和)[2] WANG Yu(王宇)[2] ZHAO Zhong-Yi(赵仲毅)[2,3] FU Yan-Hong(付艳红)[2,3]
ZHANG Ya(张娅)[2,3] MA Ke-Yan(马克岩)[1] CHEN Yong(陈勇)[2;1)]

[1] College of Physics, Jilin University, No.2699, Qianjin Road, Changchun 130023, China
[2] Key Laboratory of Particle Astrophysics, Institute of High Energy Physics, Chinese Academy of Sciences, 19B Yuquan Road, Beijing 100049, China
[3] School of Physical Science and Technology, Yunnan University, Cuihu North Road 2, Kunming 650091, China

Abstract: Readout noise is a critical parameter for characterizing the performance of charge-coupled devices (CCDs), which can be greatly reduced by the correlated double sampling (CDS) circuit. However, a conventional CDS circuit inevitably introduces new noise since it consists of several active analog components such as operational amplifiers. This paper proposes a digital CDS circuit technique, which transforms the pre-amplified CCD signal into a train of digital presentations by a high-speed data acquisition card directly without the noisy CDS circuit, then implements the digital CDS algorithm through a numerical method. A readout noise of 3.3 e^- and an energy resolution of 121 eV@5.9 keV can be achieved via the digital CDS technique.

Key words: charge-coupled devices, readout noise, correlated double sampling

PACS: 29.30.Kv, 29.40.Wk, 29.85.-c **DOI:** 10.1088/1674-1137/39/7/076101

1 Introduction

Owing to their advantages of smaller size, lower power dissipation, wider response spectrum range, lower noise and higher resolution, charge-coupled devices (CCDs) have been widely applied in industrial inspection, night vision, visible imaging, soft X-ray astronomical observations and so on. As a critical parameter that has to be considered in designing and operating CCDs, noise in the CCD mainly comes from two mechanisms: one comes from the CCD itself, including shot noise, dark current noise and the transfer noise [1]; and the other comes from the operation of the CCD, such as output amplifier noise and reset noise.

It is common to suppress the reset noise with a correlated double sampling (CDS) circuit. However, traditional CDS introduces new noise, and leaves some useful information behind, e.g. the original waveform. Digital CDS, e.g. Gach J L, 2003 [2], is able to store all the initial information, which provides the possibility for variation of the backend data process. Normally the digital CDS technique introduces a method which uses the difference between the average voltage of the reference level and that of the signal level to suppress the readout noise [3]. In practice, it shows better performance in reduction of the readout noise.

In this paper, a digital correlated double sampling circuit technique is proposed. A PCI-9846H data acquisition card, which is manufactured by ADLINK Inc., has been used to convert the pre-amplified CCD signal into a digital representation. The digital CDS system can record a large amount of data and the original waveform can be derived from these data to further analyze the signal characteristics. So the data processing can be optimized to get better performance such as lower readout noise. The relationship between the readout noise of the digital CDS system and the sample number has been investigated. The results of the measured data show that the proposed digital CDS system is better than the conventional analog CDS system, which has been assembled on the low energy X-ray telescope (LE) of the Hard X-ray Modulation Telescope (HXMT) [4], even when the CCD operating temperature is below −110 ℃, or the CCD is degraded after irradiation by protons. Moreover, the

Received 10 October 2014, Revised 21 November 2014
∗ Supported by National Natural Science Foundation of China (10978002)
1) E-mail: ychen@mail.ihep.ac.cn

best fit value of the sampling points is determined to achieve a lower readout noise, and the correlation method is able to analyze the components of the noise.

2 Reset noise and correlated double sampling

Charge generation, collection, transfer and measurement make up all of the operations of a CCD. Taking a two-phase CCD, for example, the electronic schematic of the CCD output region is illustrated on the left part of Fig. 1; while the right part of Fig. 1 is a simple diagram of the output signal. Reset noise is generated by the periodic reset of the sense-node capacitance ($C_{\rm n}$) by the reset switch. Reset noise, $n_{\rm R}(\rm e^-)$, can be expressed as

$$n_{\rm R}(\rm e^-) = \frac{\sqrt{kTC}}{q}, \tag{1}$$

where k is Boltzmann's constant (1.38×10^{-23} J/K), T is the absolute temperature (K), C is the capacitance (F), and q is the electronic charge. Reset noise can also be called "kTC noise"[5]. The noise voltage changes very quickly when the reset switch is on, leaving an undefined level on the $C_{\rm n}$ after the switch is off. After the reset switch has turned off, the noise voltage does not change significantly over a pixel period. Reset noise can be removed or reduced by using a CDS circuit technique, which subtracts the sample taken from the signal level from the sample taken from the reference level. However, a conventional CDS circuit inevitably introduces new noise since it consists of several active analog components such as operational amplifiers. In this paper, we use a digital CDS system instead of the conventional analog CDS.

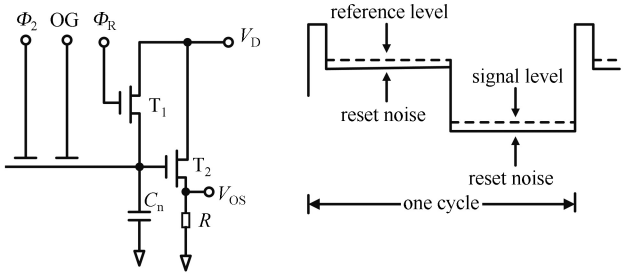

Fig. 1. Schematic of CCD output region and output signal.

3 Brief introduction to the experiment equipment

3.1 Target CCD detector

The CCD detector discussed in this paper is a CCD236. It is a two-phased swept charge device (SCD) which was designed by E2V Inc. for HXMT-LE, in collaboration with the Institute of High Energy Physics (IHEP). CCD236 achieves a high transfer rate by abandoning the position information of the X-ray photons. Charges are first transferred to the electrodes on the diagonal perpendicular to the electrodes, and then to the read-out section, which is located in the center of the chips, along the diagonal. Besides the real output, there is a dummy output that is the same as the real one. As the dummy output only carries common-mode noise, the negative effect of common-mode noise can be greatly suppressed by subtracting that noise from the real output signal [6].

3.2 Data acquisition card

The PCI-9846H is a data acquisition card manufactured by ADLINK inc., designed for digitizing high frequency and wide dynamic range signals, taking advantage of its rapid read-out speed and lower system noise. Its onboard 512 MB acquisition memory enables it to store the data of the waveform for a considerable time. It has a high linearity 16-bit A/D converter, and a sampling rate up to 40 million samples per second (MS/s). In addition, the analog voltage range is ±5 V [7].

3.3 Digital CDS readout system

The digital CDS system block diagram is shown in Fig. 2, and is made up of three parts: pre-amplifier, voltage buffer and data acquisition system. The voltage gain of the pre-amplifier is 11. The voltage buffer ensures the accuracy of the signal amplitude. The PCI-9846H digitizes the analog input at a certain rate, and sends the conversion results to the computer via PCI (peripheral component interconnection) for backend data processing.

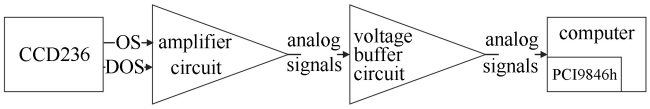

Fig. 2. The digital CDS system block diagram.

4 Results of performance testing

4.1 Test results at low CCD operating temperature

To investigate the performance of the digital CDS system, a test has been carried out with the CCD operated below about −110 ℃, as the effect of the dark current from the CCD can be ignored at such a low temperature. The driving clock for the CCD is 83.3 kHz, while the digital data acquisition system is sampling at 40 MS/s (million samples per second). An ^{55}Fe radioactive source was used to measure the energy resolution.

As shown in Fig. 3, the waveform is reconstructed from a total of 480 sample points. Due to such non-idealities as clock feed-through, parasitic effects as well as signal integrity problems, glitches are prominent at the edges of the driving clocks. However, only the two steady parts of every cycle make sense, since signals in these two parts are completely settled. A certain number of sample points are selected as effective points for processing.

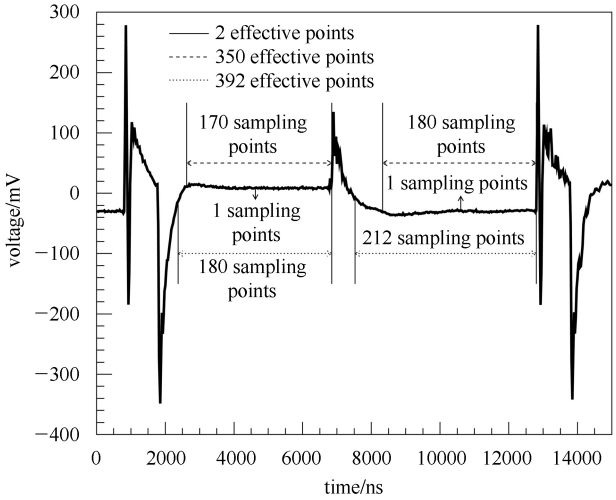

Fig. 3. Typical signal waveform.

The flat section of the curve in Fig. 3 is selected on the basis of the difference of the voltage between two adjacent sampling points being no more than 40 mV. Taking the section of the signal level as an example, the initial point (the 389th point) is exactly placed in the middle of the flat section, the second one is located just to the left of the initial one (i.e. the 388th point), the third one is situated just to the right of the initial one (i.e. the 390th point), and so on. All the points right of the 477th point are ignored. The way to select points on the reference level is just the same, and the initial point in this case is the 150th point. During the following numerical calculation, the number of effective points increases from 2 to 392 in order to find out the optimal number. Eventually, the voltage amplitude of the incoming X-ray photons can be obtained by the equation

$$V_{\rm ph} = \overline{V_{\rm Ref}} - \overline{V_{\rm Signal}}, \tag{2}$$

where $\overline{V_{\rm Signal}}$ is the average voltage of the sampling points on the flat section of the signal level, and $\overline{V_{\rm Ref}}$ is the average voltage of the sampling points on the flat section of the reference level.

As shown in Fig. 4, below 350 samples, the readout noise decreases with the effective points increasing. The function (Eq. (2)) has been used to fit the relationship between the readout noise and the number of effective

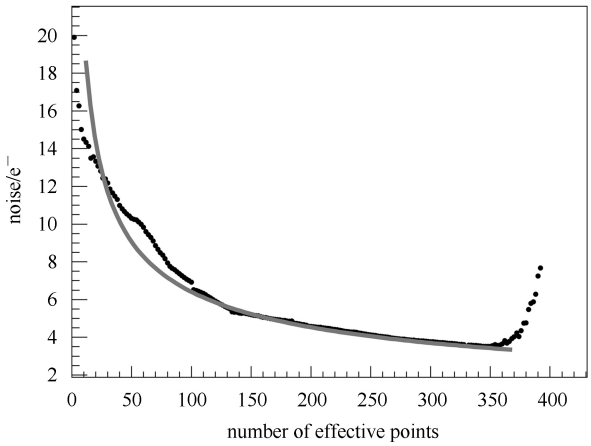

Fig. 4. Readout noise vs. number of effective sampling points under 83.3 kHz operating frequency.

sampling points, which describes the error of the mean value for the independent sampling data.

We try to use Eq. (3) to fit the data in Fig. 4:

$$n = \frac{A_0}{\sqrt{N}}, \tag{3}$$

where n is readout noise (e^-), and N is the number of effective sampling points. The fitting curve is shown in Fig. 4 as the solid line, with the value of A_0 (64.1±0.6) e^-. When only one point is sampled on each level ($N=2$), the noise is about 20 e^-, which is significantly lower than the value of the reset noise (53 e^-) calculated by Eq. (1), where C is 0.032 pF for CCD236 and T is 160 K. However, the declination of the data in Fig. 4 indicates that there are also other sources of noise or interferences besides the reset noise.

Eq. (3) cannot fit the data well at both ends. In detail, the readout noise increases again when the number of effective points exceeds 350, because the data beyond the steady parts are used. The ranges of 350, 392 effective points are shown in Fig. 3. Obviously, the optimal effective point number is around 350, so we select this number in all the tests below in this paper. As the sampling points are fewer, shown in the left-hand side of Fig. 4, the declining slope of the data is significantly shallower than $1/\sqrt{N}$. It is suggested that the sampling data are not independent in this situation.

We calculated the cross-correlation function of the voltage of each sampling point and the initial sampling point (i.e. the 389th point). As shown in Fig. 5, sampling points located far away from each other are weakly correlated, while adjacent sampling points show sharp oscillation, from strongly correlated to anti-correlated. It indicates that the readout noise is probably not white noise.

For this purpose, the power spectrum of the readout noise (the part of the signal level) is calculated by the

fast Fourier transform (FFT) method. In the power spectrum (Fig. 6), there is substantial low-frequency noise, most likely $1/f^{\alpha}$ noise with α from 1 to 2. The lower frequency noise component may be responsible for the weak correlation at long distance. On the other hand, it is found that there is an enhancement at about 5 MHz in the power spectrum, which can explain the strong correlation at short distance. The lower frequency noise may come from the onchip field effect transistor (FET) of the CCD readout circuit[8], and the ∼5 MHz noise is probably caused by outside interference or the CCD itself.

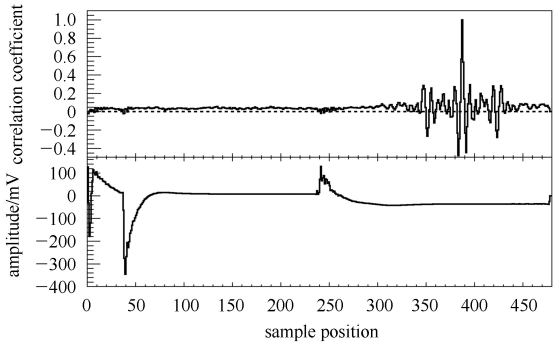

Fig. 5. Cross-correlation between the voltages of each sampling point and the initial sampling point (the 389th point). The upper plot is the cross-correlation data, and the lower plot is the mean value of the waveform for reference.

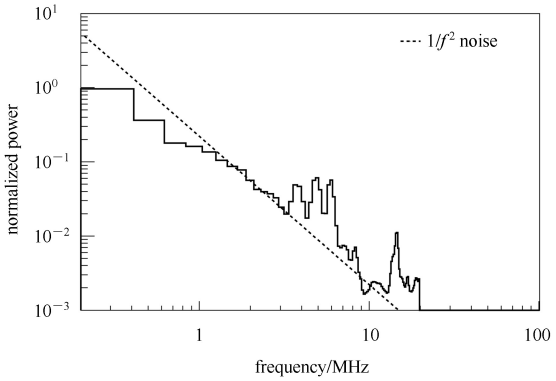

Fig. 6. The normalized power spectrum of the readout noise in the part of the signal level, with a $1/f^2$ noise shown as a dashed line for reference.

To determine the performance, especially the energy linearity, an X-ray tube with a copper target is used. From the spectrum which is shown in Fig. 7, four distinct peaks besides the noise peak are found. The integral nonlinearity (INL) is satisfactory, with a value of 0.4%.

To investigate the energy resolution of the system, a test was conducted with an ^{55}Fe radioactive source. The spectrum is shown in Fig. 9. Fitting the noise peak and Mn K_{α} (5.9 keV) peak by Gaussians, the mean value and the standard deviation can be obtained, and the energy resolution of the CCD detector system is calculated to be 121.0±0.4 eV@5.9 keV (FWHM), and the readout noise is (3.342±0.002) e^-.

Within the temperature range of −116 ℃ to −110 ℃, the readout noise and energy resolution of the digital CDS system and the conventional CDS readout system under the same condition are compared in Table 1, which illustrates that the performance of the digital CDS system is better than that of the conventional CDS system.

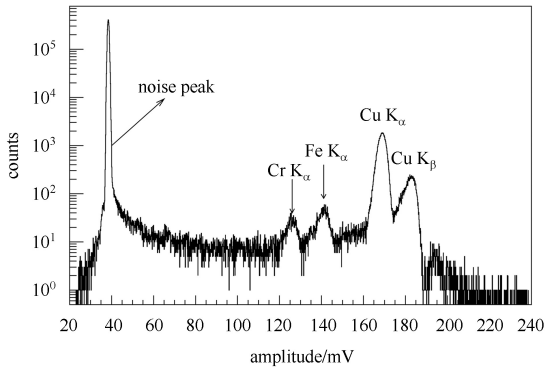

Fig. 7. Spectrum from a copper target bombarded with X-rays generated by an X-ray tube.

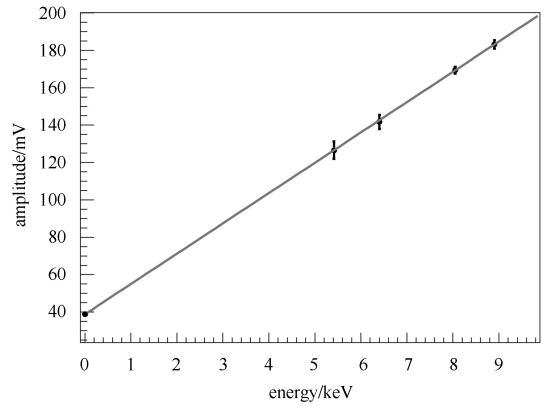

Fig. 8. Integral nonlinearity of the digital CDS system.

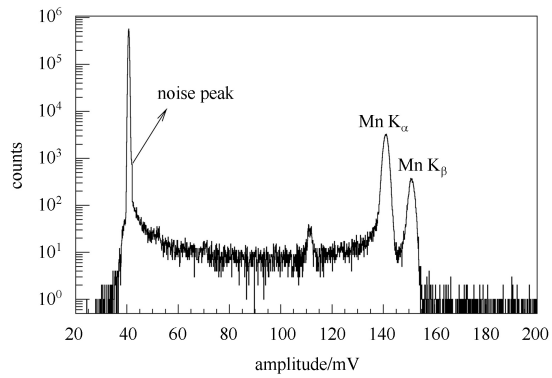

Fig. 9. An ^{55}Fe spectrum of CCD236 at −113 ℃.

Table 1. Performance comparison between digital and analog CDS systems.

CCD operational	energy resolution(FWHM)/eV		readout noise/e^-	
temperature/℃	digital CDS system	conventional CDS system	digital CDS system	conventional CDS system
−110.3	123.4±0.4	131.9±1.1	3.487±0.002	5.251±0.002
−113.0	121.0±0.4	131.0±1.1	3.342±0.002	5.428±0.002
−115.1	121.7±0.4	131.4±1.1	3.331±0.002	5.208±0.002
−116.2	121.3±0.4	129.7±1.0	3.329±0.002	5.416±0.002

4.2 Performance comparison between two systems after proton irradiation

The readout noise and energy resolution of a proton-irradiated CCD236, with a dose of 3×10^8 p/cm^2, are measured with the temperature ranging from −60 ℃ to −10 ℃ [9].

As shown in Fig. 10, the readout noise of the digital CDS system is about 2 e^- lower than that of the conventional CDS readout system in the temperature range from −60 ℃ to −30 ℃. The difference in readout noise gradually increases to 4 e^- when the temperature warms up to −10 ℃. In addition, the energy resolution of the digital CDS system also shows a similarly better result (Fig. 11). The performance of the digital CDS system is better than the conventional CDS system after proton irradiation. Therefore, it is a promising way to suppress the negative effects of the proton-irradiation damage to the CCDs.

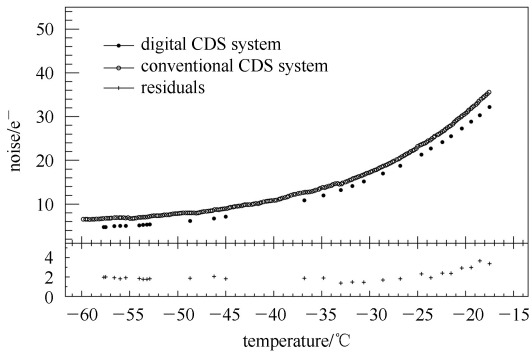

Fig. 10. Comparison of the readout noise. The open circles, solid circles and plus signs ('+') represent the data of the conventional CDS system, the digital CDS system and the residuals, respectively.

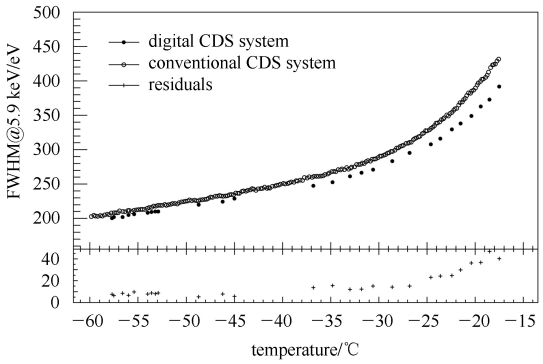

Fig. 11. Comparison of the energy resolution. The open circles, solid circles and plus signs ('+') represent the data of the conventional CDS system, the digital CDS system and the residuals, respectively.

5 Conclusions

In this paper, we have proposed a digital CDS system. Under the same conditions, the readout noise is reduced monotonically as the number of sampling points per cycle increases to a certain number (350 in this paper). From the waveform obtained from the digital CDS system, we have analysed the sources of noise by the power spectrum. Compared to the conventional CDS system, the digital CDS system has a lower readout noise and a better energy resolution, not only under very low CCD operating temperatures but also proton-irradiation. Additionally, the digital CDS system shows a satisfactory INL. In summary, digital CDS is a promising technique to reduce the readout noise of CCDs, to suppress the effect of interference, and to investigate the properties of noise.

References

1 ZHANG Jun-Min, XU Yu-Peng, CHEN Yong et al. Journal of Chinese Inertial Technology, 2009, **17(6)**: 666–669 (in Chinese)
2 Gach J L, Darson D, Guillaume C et al. The Astronomical Society of the Pacific, 2003, **115**: 1068–1071
3 Fowler A M, Gatley I. The Astrophysical Journal, 1990, **353**: L33–L34
4 LI Ti-Pei. Nuclear Physics B Proceedings Supplements, 2007, **166**: 131–139
5 Janesick J R. Scientific Charge-Coupled Devices. Bellingham, Washington: SPIE Press, 2001. 537–538
6 WANG Yu-Sa, CHEN Yong, XU Yu-Peng et al. Chinese Physics C, 2009, **33(X)**: 1–5
7 http://www.adlinktech.com/PD/marketing/Datasheet/ PCI-9816+9826+9846/PCI-9816+9826+9846_Datasheet_en_1.pdf
8 Centen P. IEEE Trans. Electron Devices, 1991, **38**: 1206–1216
9 YANG Yan-Ji, LU Jing-Bin, WANG Yu-Sa et al. Chinese Physics C, 2014, **38(8)**: 086004